Available online at www.sciencedirect.com
SCIENCE DIRECT
Applied Catalysis B: Environmental 57 (2005) 283–290
APPLIED CATALYSIS B: ENVIRONMENTAL
www.elsevier.com/locate/apcatb

Carbon supported Pt–Co alloys as methanol-resistant oxygen-reduction electrocatalysts for direct methanol fuel cells

José Ricardo Cezar Salgado[a], Ermete Antolini[a,b,*], Ernesto Rafael Gonzalez[a]

[a]*Instituto de Química de São Carlos, USP, C.P. 780, São Carlos, SP 13560-970, Brazil*
[b]*Scuola di Scienza dei Materiali, Via 25 Aprile 22, 16016 Cogoleto, Genova, Italy*

Received 28 June 2004; received in revised form 5 November 2004; accepted 11 November 2004
Available online 22 December 2004

Abstract

The electrocatalysis of the oxygen reduction reaction on carbon supported Pt and Pt–Co (Pt/C and Pt–Co/C) alloy electrocatalysts was investigated in sulphuric acid (both in the absence and in the presence of methanol) and in direct methanol fuel cells (DMFCs). In pure sulphuric acid Pt–Co/C alloys showed improved specific activity towards the oxygen reduction compared to pure platinum. In the methanol containing electrolyte a higher methanol tolerance of the binary electrocatalysts than Pt/C was observed. The onset potential for methanol oxidation at Pt–Co/C was shifted to more positive potentials. Accordingly, Pt–Co/C electrocatalyts showed an improved performance as cathode materials in DMFCs.

Keywords: Pt–Co/C alloy; Oxygen reduction electrocatalyst; Direct methanol fuel cells

1. Introduction

Direct methanol fuel cells (DMFCs) are promising electrochemical energy converters for a variety of applications because of the system simplicity. The two basic electrode reactions of the DMFC are:

$$CH_3OH + H_2O \rightarrow CO_2 + 6H^+ + 6e \quad (1)$$

$$\frac{3}{2}O_2 + 6H^+ + 6e \rightarrow 3H_2O \quad (2)$$

The liquid-feed system does not require any fuel processing equipment and can be operated even at room temperatures. Another advantages of the DMFC is the fact that it does not require complex humidification and heat management modules as in the hydrogen fed proton exchange membrane (PEM) fuel cell system because the dilute methanol + water mixtures circulating around the DMFC provides the necessary humidification and heat regulation. These advantages allow the DMFC to be customized for use in portable electronic devices [1]. The major problems, which decrease the efficiency of conversion of the chemical energy of the methanol fuel to electrical energy in a DMFC, are the slow methanol electrooxidation reaction kinetics at conventional Pt anode electrocatalysts and the methanol crossover through the polymer electrolyte. The poor kinetics of methanol oxidation at the anode is mostly due to self-poisoning of the surface by reaction intermediates such as CO, which are formed during dehydrogenation of the methanol [2]. Therefore, in order to improve the efficiency of the DMFC, anode electrocatalysts are required which combine a high activity for methanol dehydrogenation and an improved tolerance towards CO poisoning [3–6].

Additionally, as it is well known, when two solutions of different concentrations are separated by a membrane, a diffusion of the solute takes place across the membrane from the more concentrated to the more dilute solution. This transport process gives rise to one of the major chemical problems in direct methanol fuel cells, where a difference of methanol concentration exists between the anodic and the cathodic compartments. The methanol transport through

* Corresponding author. Tel.: +55 16 3373 9951/+39 010 916 2880; fax: +55 16 3373 9952/+39 010 918 2368.
E-mail address: ermantol@libero.it (E. Antolini).

0926-3373/$ – see front matter © 2004 Elsevier B.V. All rights reserved.
doi:10.1016/j.apcatb.2004.11.009

perfluorosulphonate membranes, which typically happens in direct methanol fuel cells, and is usually known as methanol crossover, occurs by diffusion as a result of the concentration gradient and also due to electro-osmotic drag. The problem of methanol crossover in DMFCs has been extensively studied [7–11]: methanol adsorbs on Pt sites in the cathode for the direct reaction between methanol and oxygen. The mixed potential, which results from the oxygen reduction reaction and the methanol oxidation occurring simultaneously, reduces the cell voltage, generates additional water and increases the required oxygen stoichiometric ratio. This problem could be solved either by using electrolytes with lower methanol permeability or by developing new cathode electrocatalysts with both higher methanol tolerance and higher activity for the oxygen reduction reaction (ORR) than Pt. Higher methanol tolerance is reported in the literature for non-noble metal electrocatalysts based on chalcogenides [12–15] and macrocycles of transition metals [16,17]. These electrocatalysts have shown nearly the same activity for the ORR in the absence as well as in the presence of methanol. However in methanol free electrolytes, these materials did not reach the catalytic activity of dispersed platinum. Developing a sufficiently selective and active electrocatalyst for the DMFC cathode remains one of the key tasks for further progress of this technology.

The alloys of transition metals, such as V, Cr, Co, Ti and Ni, with platinum have been found to exhibit higher electrocatalytic activities towards the ORR than platinum alone in low temperature fuel cells [18–30]. The improvement in the ORR electrocatalysis has been ascribed to different factors such as changes in the Pt–Pt interatomic distance [19], the surface area [26] and the d-orbital vacancy [23]. According to different authors [31,32], among the various alloy electrocatalysts investigated, Pt–Co/C showed the higher catalytic activity for the ORR. The current direction is to test the activity for the ORR of these materials in the presence of methanol. An enhanced electrocatalysis for the ORR in the presence of methanol at Pt–Ni [33] and Pt–Cr [34] alloy electrocatalysts was observed by rotating disk electrode measurements. By polarization data in DMFCs Shukla et al. [35] found that Pt–Fe is an effective methanol-resistant oxygen reduction electrocatalyst. Neergat et al. [36] ascribed the superior activity of carbon supported Pt–Co in the Pt:Co atomic ratio 1:1 as oxygen-reduction electrocatalyst in DMFCs, relative to Pt/C and other alloy electrocatalysts, to the enhanced oxygen reduction kinetics [36].

On these bases, the purpose of the present work is to provide evidence of the effect of cobalt on the tolerance towards methanol oxidation of Pt-based carbon supported electrocatalysts for oxygen reduction. Pt/C and Pt–Co/C electrocatalysts are compared for the ORR in the presence and in the absence of methanol, and for the methanol oxidation reaction (MOR). Their performances as cathode materials in single DMFC experiments are also compared.

2. Experimental

2.1. Preparation of carbon supported Pt–Co electrocatalysts

Carbon supported Pt–Co electrocatalysts in the nominal Pt:Co atomic ratio 75:25 were prepared by the borohydride method and the alloying method.

Borohydride method (BM): The electrocatalyst was prepared by impregnating high surface area carbon with a chloroplatinic acid solution and a cobalt hydroxide ($Co(OH)_2{\cdot}6H_2O$, Aldrich) solution. The metals were then reduced with a sodium borohydride solution, which was slowly added under sonication.

Alloying method (AM): The required amount of E-TEK 20 wt.% Pt/Vulcan XC-72 (particle size 2.8 nm) was dispersed in distilled water followed by ultrasonic blending for 15 min. The pH of the solution was raised to 8 with dilute ammonium hydroxide. Stirring was continued during and after the pH adjustment. The required amount of a solution of cobalt chloride ($CoCl_2{\cdot}6H_20$, Aldrich) was added to this solution. This was followed by the addition of dilute HCl to the solution until a pH of 5.5 was attained. Stirring was continued for 1 h and the resultant mass was filtered and dried at 90 °C in an air oven for 2 h. Subsequently, the solid was well grinded and the powder was heat-treated at 900 °C in a hydrogen/argon atmosphere for 1 h to form the respective binary alloy catalyst.

The materials prepared by the borohydride method were 20 wt.% metal on carbon, while those prepared by the alloying method were 22 wt.% metal on carbon.

2.2. Physical characterization of Pt/C and Pt–Co/C electrocatalysts

The atomic ratios of the Pt–Co/C electrocatalysts were determined by energy dispersive X-ray analysis (EDX) coupled to a scanning electron microscopy LEO Mod. 440 with a silicon detector with Be window and applying 20 keV.

X-ray diffractograms of the electrocatalysts were obtained in a universal diffractometer Carl Zeiss-Jena, URD-6, operating with Cu Kα radiation ($\lambda = 0.15406$ nm) generated at 40 kV and 20 mA. Scans were done at $3^\circ\ min^{-1}$ for 2θ values between 20 and 100°. In order to estimate the particle size from XRD Scherrer's equation was used [37]. For this purpose, the (2 2 0) peak of the Pt fcc structure around $2\theta = 70^\circ$ was selected. In order to improve the fitting of the peak, recordings for 2θ values from 60 to 80° were done at $0.02^\circ\ min^{-1}$. The lattice parameters were obtained by refining the unit cell dimensions by the least squares method [38].

The samples for the TEM characterizations were prepared as follows: a carbon film was deposited onto a mica sheet that was placed onto the Cu grids (300 mesh and 3 mm diameter). The material to be examined was dispersed in water by sonication, placed onto the carbon film and left to

Table 1
Structural characteristics of Pt–Co/C and commercial Pt/C electrocatalyts

Catalyst	EDX composition	Lattice parameter (nm)	Particle size (XRD) (nm)	Particle size (TEM) (nm)	Surface area from CV ($m^2\ g^{-1}$)	Roughness factor ($cm^2\ cm^{-2}$)
PtCo by AM	75:25	0.3841	4.6	3.9	48	480
PtCo by BM	85:15	0.3874	3.8	3.7	50	500
Pt/C	100	0.3915	2.8	3.0	95	950

dry. Histograms of particle sizes were constructed using about 500 particles.

2.3. Electrode preparation and electrochemical characterization of Pt/C and Pt–Co/C electrocatalysts

In order to test the electrochemical behaviour in sulphuric acid (with and without methanol) and in a single DMFC fed with methanol/oxygen, the electrocatalysts were used to make two layer gas diffusion electrodes (GDE). A diffusion layer was made with carbon powder (Vulcan XC-72) and 15 wt.% polytetrafluoroethylene (PTFE) and applied over a carbon cloth (PWB-3, Stackpole). On top of this layer, the electrocatalyst was applied in the form of a homogeneous dispersion of Pt–Co/C, or Pt/C, Nafion® solution (5 wt.%, Aldrich) and isopropanol (Merck) [39]. All electrodes were made to contain 1 mg Pt cm^{-2}.

Cyclic voltammograms were recorded in a single cell in 0.5 mol L^{-1} H_2SO_4 solution. Argon (White Martins) was passed for 30 min to eliminate oxygen. Gas diffusion electrodes containing Pt/C and Pt–Co/C electrocatalysts were used as working electrodes. A hydrogen electrode was used as reference and a platinum foil electrode as auxiliary. The CV's were recorded in the range 0.075–0.800 V versus a reversible hydrogen electrode (RHE) at a scan rate of 20 mV s^{-1}.

The electrochemical half-cell was built in PTFE with a volume of approximately 70 mL. After the voltammetric study, oxygen was passed for 30 min to saturate the solution. The current-potential curves for the ORR were registered in the absence and in the presence of different amounts of methanol. Linear sweep curves were recorded in the range of 0.1–1.0 V versus a RHE. The oxidation of methanol on Pt–Co/C and Pt/C was tested in 0.5 and 3 mol L^{-1} methanol solutions. The experiments were done at room temperature with a 1285A Solartron Potentiostat connected to a personal computer and using the software CorrWare for Windows (Scribner).

For the direct methanol single cells studies, the electrodes were hot pressed on both sides of a Nafion® 117 membrane at 125 °C and 50 kg cm^{-2} for 2 min. In the case of the membrane/electrodes assembly with the $Pt_{85}Co_{15}$/C electrocatalyst, a Nafion 115 membrane was used. Before using them, the Nafion® membranes were treated with a 3 wt.% solution of H_2O_2, washed and then treated with a 0.5 mol L^{-1} solution of H_2SO_4. The geometric area of the electrodes was 4.62 cm^2, and the anode material was 20 wt.% $Pt_{80}Ru_{20}$/C. The cell polarization data at 90 °C were obtained by circulating a 2 mol L^{-1} aqueous methanol solution at the anode and oxygen at 3 atm pressure at the cathode.

3. Results and discussion

The compositions for the carbon supported Pt–Co electrocatalysts are given in Table 1. As can be seen in Table 1, the composition of Pt–Co by the alloying method corresponds to the nominal value, while that of Pt–Co by the borohydride method was 85:15. On this basis, the electrocatalyst prepared by the alloying method will be identified as $Pt_{75}Co_{25}$/C, and the electrocatalyst prepared by the borohydride method as $Pt_{85}Co_{15}$/C. Fig. 1 shows the X-ray diffraction patterns of Pt/C and Pt–Co/C alloy electrocatalysts. As indicated in Fig. 1, all the XRD patterns clearly show the five main characteristic peaks of the face-centered cubic (fcc) crystalline Pt, namely, the planes (1 1 1), (2 0 0), (2 2 0), (3 1 1), and (2 2 2). These five diffraction peaks in the Pt–Co/C alloy electrocatalysts are slightly shifted to higher angles with respect to the corresponding peaks in the Pt/C electrocatalyst, indicating a contraction of the lattice and alloy formation. No peak for pure Co and its oxides was found, but their presence cannot be discarded because they may be present in a very small amount or even in an amorphous form. In addition to the five main characteristic peaks of the Pt fcc structure, three weak peaks were found for the $Pt_{75}Co_{25}$/C electrocatalyst, which were assigned to the superlattice planes of an ordered Pt–Co alloy phase. The lattice parameters of Pt/C and Pt–Co/C alloy electrocatalysts are reported in Table 1. The obtained

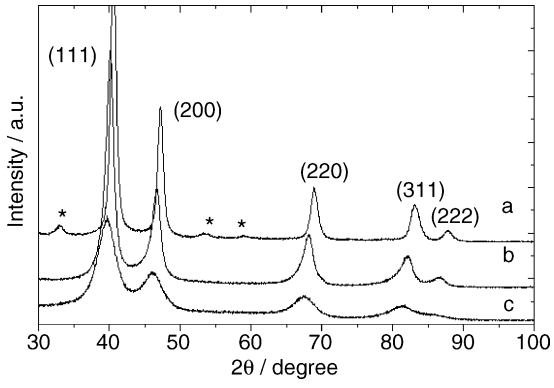

Fig. 1. XRD diffractograms of $Pt_{75}Co_{25}$/C (a) and $Pt_{85}Co_{15}$/C (b) and commercial Pt/C (c) electrocatalysts.

lattice parameters for all the Pt–Co/C alloy electrocatalysts are smaller than those for Pt/C and decrease with the increase of Co content, reflecting a progressive introduction of Co into the alloyed state. Also the diffraction peaks of the binary electrocatalysts are sharper than those in pure platinum indicating a larger metal particle size. The sizes of the carbon supported particles determined with XRD and TEM are reported in Table 1.

Fig. 2 shows the TEM images of the carbon-supported commercial Pt and the as-prepared Pt–Co/C alloy electrocatalysts. The corresponding particle size distribution histograms are reported in Fig. 3. As can be seen, the commercial Pt/C presents a somewhat better dispersion on the carbon support. Moreover, the Pt–Co/C alloy nanoparticles tend to form aggregates. Both Pt–Co/C samples present a broader particle size distribution than Pt, with a tail in the region of larger particles. The average particle sizes calculated by TEM are consistent with those obtained by XRD, as shown in Table 1.

Fig. 4 shows cyclic voltammograms (CV) performed in a single polymer electrolyte fuel cell operating with hydrogen for Pt/C and Pt–Co/C electrocatalysts. From the hydrogen adsorption peak areas in the CV curves, and considering a charge of 210 C cm^{-2} Pt for a monolayer of hydrogen adsorbed on polycrystalline Pt, the electrochemical surface areas for the electrocatalysts were calculated. As shown in Table 1, the electrochemical surface area of Pt/C is about twice the value of the binary electrocatalysts.

The experimental results regarding the ORR in H_2SO_4 solution are shown in Fig. 5(a). Here the current density is expressed in terms of mass activity (MA), being the Pt loading 1 mg cm^{-2} for all the electrodes and in terms of the geometric surface area. In Fig. 5(b) the current density is expressed in terms of the real surface area of platinum calculated from the hydrogen desorption regions of the CV, i.e. in terms of specific activity (SA). The onset potential for the ORR is the same for Pt and Pt–Co/C electrocatalysts at about 850 mV. In terms of mass activity the slope of the current density–potential plot, (dj/dE), of Pt/C is slightly higher than that of the Pt–Co/C electrocatalysts. On the other hand, on the basis of the specific activity, dj/dE increases with increasing Co content in the electrocatalyst.

Fig. 6(a)–(c) shows the ORR activity of the prepared Pt–Co/C alloy electrocatalysts and the Pt/C electrocatalyst in the presence of various methanol concentrations, from 0 to 3 mol L^{-1} CH_3OH. As can be seen, all the electrocatalysts show an increase in overpotential for the ORR (both with respect to MA and SA) under the same current density in the presence of methanol. From Fig. 6, it is evident that the methanol tolerance is higher for Pt–Co/C electrocatalysts. Passing from H_2SO_4 to $H_2SO_4 + CH_3OH$, up to a concentration of 1 M CH_3OH the change in dj/dE for Pt–Co catalysts is lower than that for pure Pt (0.05, 0.08 and 0.14 mA V^{-1} for $Pt_{85}Co_{15}$/C, $Pt_{75}Co_{25}$/C and Pt/C, respectively). Thus, it can be inferred that Pt–Co alloy catalysts are less affected by the presence of methanol. Above 1 M CH_3OH, the change in dj/dE is about the same for all the catalysts. The higher methanol tolerance of Co-containing catalysts with respect to that of Pt alone can be more clearly seen in Fig. 7, where the potentials at 0.1 mA cm^{-2}

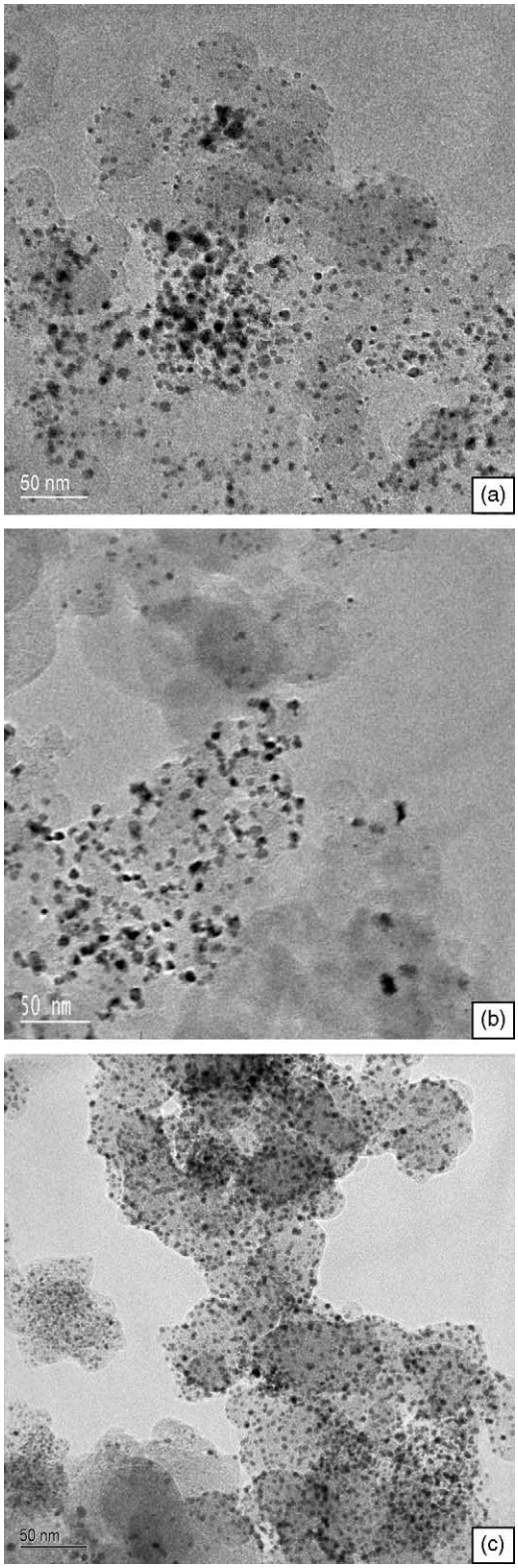

Fig. 2. TEM images of $Pt_{75}Co_{25}$/C (a), $Pt_{85}Co_{15}$/C (b) and commercial Pt/C (c) electrocatalysts. Magnification 50.000.

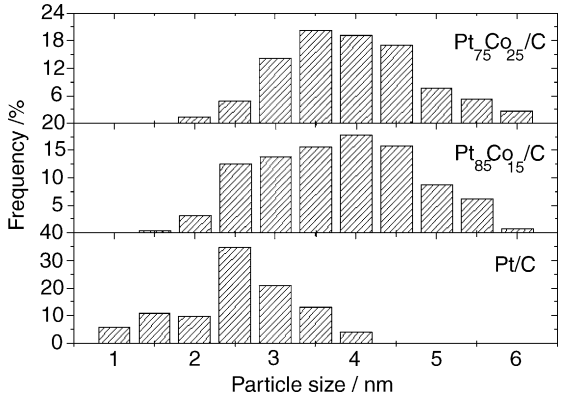

Fig. 3. Histograms of Pt particle size distribution in the Pt–Co/C and commercial Pt/C electrocatalysts.

($E_{0.1\,mA\,cm^{-2}}$) from Fig. 6 (the choice of this value of current density in the region of oxygen reduction is arbitrary, being the trend similar for all the values of current density) are plotted against methanol concentration. The decrease of $E_{0.1\,mA\,cm^{-2}}$ on the Pt/C electrocatalyst with increasing methanol concentration is much higher than that on the alloys, showing that the Pt–Co/C electrocatalysts have a better tolerance to the presence of methanol than Pt/C in pure sulphuric acid solution.

The linear scan voltammograms for the methanol oxidation on the Pt/C electrocatalyst and the carbon supported Pt–Co alloy electrocatalysts in nitrogen saturated 1 mol L^{-1} H_2SO_4/3 mol L^{-1} CH_3OH are shown in Fig. 8. The methanol-containing electrolyte was previously purged with nitrogen in order to avoid oxygen contamination. It can be seen that the current densities for the methanol oxidation reaction on the Pt–Co/C alloy electrocatalysts are much lower than that on the Pt/C electrocatalyst and that the onset potential for methanol oxidation on the Pt–Co/C alloys (550 mV for $Pt_{85}Co_{15}$/C and 620 mV for $Pt_{75}Co_{25}$/C) shifts to more positive potentials as compared to Pt/C (about 500 mV), indicating again that the alloy electrocatalysts are less active than the Pt/C electrocatalyst for methanol

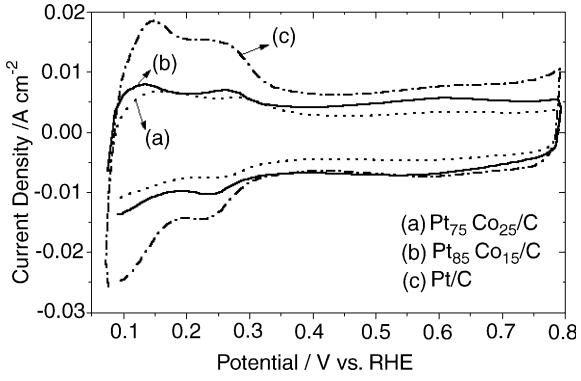

Fig. 4. Cyclic voltammograms of Pt–Co/C and commercial Pt/C electrocatalysts at room temperature in 0.5 mol L^{-1} H_2SO_4 at a scan rate of 20 mV s^{-1}.

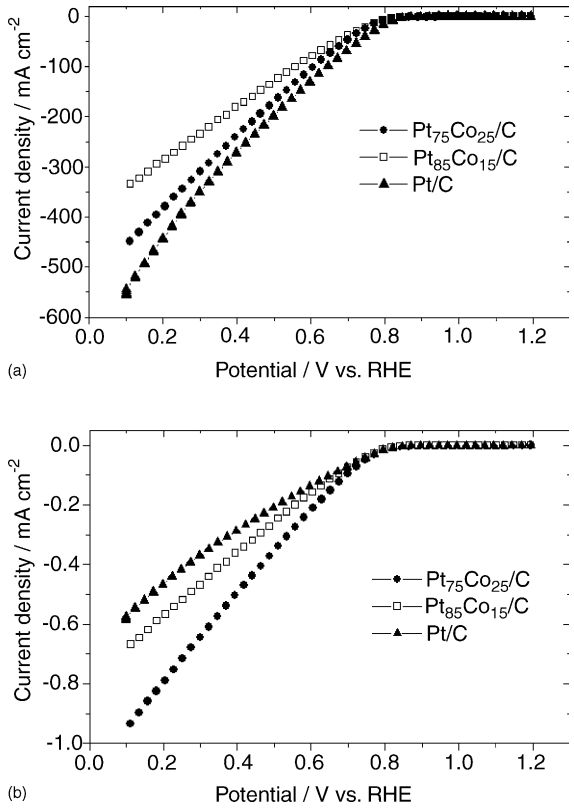

Fig. 5. Oxygen reduction at room temperature in 0.5 mol L^{-1} H_2SO_4 on Pt–Co/C and Pt/C electrocatalysts. (a) Current densities normalized with respect to the geometric surface area (MA); (b) current densities normalized with respect to the Pt surface area (SA).

oxidation. This fact could also explain the high methanol tolerance of the Pt–Co/C alloy electrocatalysts. Maillard et al. [40] found that electrocatalysts for the ORR with small metal particle size have enhanced methanol tolerance. In this case, the higher methanol-tolerance of the binary electrocatalysts cannot be ascribed to a particle size effect, being the particle size of Pt smaller than those of the Pt–Co/C materials. It is believed that methanol adsorption and oxygen adsorption are competing with each other for the surface sites. Also, it is well established that for methanol oxidation at least three adjacent Pt sites in the proper crystallographic arrangement are necessary to activate the chemisorptions of methanol [3,41–43]. For the Pt–Co/C alloy electrocatalysts, the probability of finding three neighbouring Pt atoms on the surface is lower if no Pt enrichment of the surface takes place. Since the dissociative chemisorption of methanol requires several adjacent Pt ensembles, the presence of methanol-tolerant Co around Pt active sites could hinder methanol adsorption on Pt sites due to the dilution effect. On the other hand, oxygen adsorption, which usually can be regarded as dissociative chemisorption and requires only two adjacent Pt sites, is not influenced by the presence of Co atoms. It is interesting to note that both the current density in Fig. 8 and the change in dj/dE in the presence of methanol in Fig. 6 are lower for the $Pt_{85}Co_{15}$ alloy than for the $Pt_{75}Co_{25}$

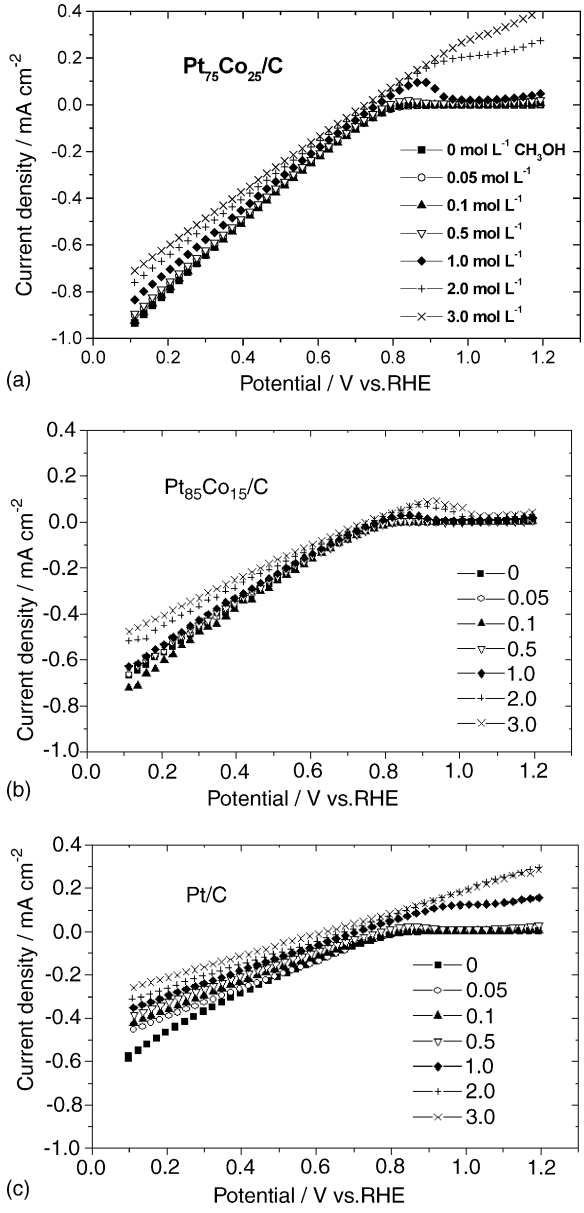

Fig. 6. Oxygen reduction at room temperature in 0.5 mol L^{-1} H_2SO_4 containing different amounts of methanol. $Pt_{75}Co_{25}$/C (a), $Pt_{85}Co_{15}$/C (b) and commercial Pt/C (c) electrocatalysts. Current densities normalized with respect to the Pt surface area (SA).

alloy catalyst. This result, notwithstanding the higher Co content further decreases the probability of finding neighboring Pt atoms for methanol chemisorption, as attested by the values of the onset potential for the MOR, can be explained on the basis of the electronic effect of Co on the occupancy of the Pt 5 d-band. Indeed, the strong adsorption of OH and CO on small particles (<5 nm) hinders methanol oxidation, as a result of a significant increase in the Pt 5 d-band vacancy [44]. But a decrease in Pt d-band vacancy occurs by increasing the content of the non-precious metal in the alloy [45], supporting in this way the MOR activity of the catalyst. Thus, the alloy with a higher Co content becomes less methanol resistant.

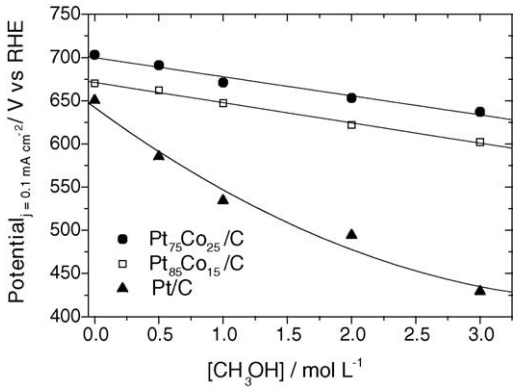

Fig. 7. Dependence of the potential at 0.1 mA cm^{-2} ($E_{0.1\,mA\,cm^{-2}}$) during O_2 reduction in 0.5 mol L^{-1} H_2SO_4 on methanol concentration.

The polarization curves in single DMFC with Pt/C and Pt–Co/C as cathode electrocatalysts and $Pt_{80}Ru_{20}$/C as anode material operating with 2 mol L^{-1} methanol solution at 90 °C and a cathode pressure of 3 atm are shown in Fig. 9(a) (in MA). As described in the experimental part, unlike the cell with Pt/C and $Pt_{75}Co_{25}$/C, made with a 117 Nafion membrane, for the cell with $Pt_{85}Co_{15}$/C a 115 (thinner) Nafion membrane was used. The best cell performance was obtained with the cell employing the $Pt_{75}Co_{25}$/C electrocatalyst. The performance of the cell with the $Pt_{85}Co_{15}$/C cathode was poorer than that with Pt/C at low current densities, and better than pure platinum at high current densities. This behaviour is related to the use of a thinner membrane. Indeed, according to Heinzel and Barragan [9], the methanol crossover increases and the cell performance at low current density decreases with decreasing membrane thickness. On the basis of the SA, a larger improvement of the cell performance was observed with Co-containing electrocatalysts with respected to Pt/C, as shown in Fig. 9(b). These results indicate that Pt–Co/C alloy electrocatalysts have better activities for the ORR in the presence of methanol than Pt/C both in pure sulphuric acid solution and in the DMFC.

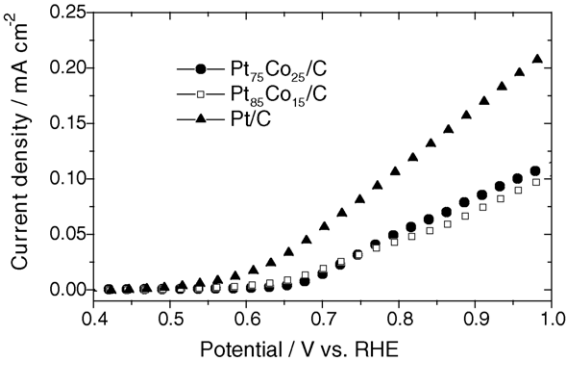

Fig. 8. Linear sweep voltammograms at room temperature for the methanol oxidation on the Pt–Co/C and Pt/C electrocatalysts in 0.5 mol L^{-1} H_2SO_4 + 3.0 mol L^{-1} methanol.

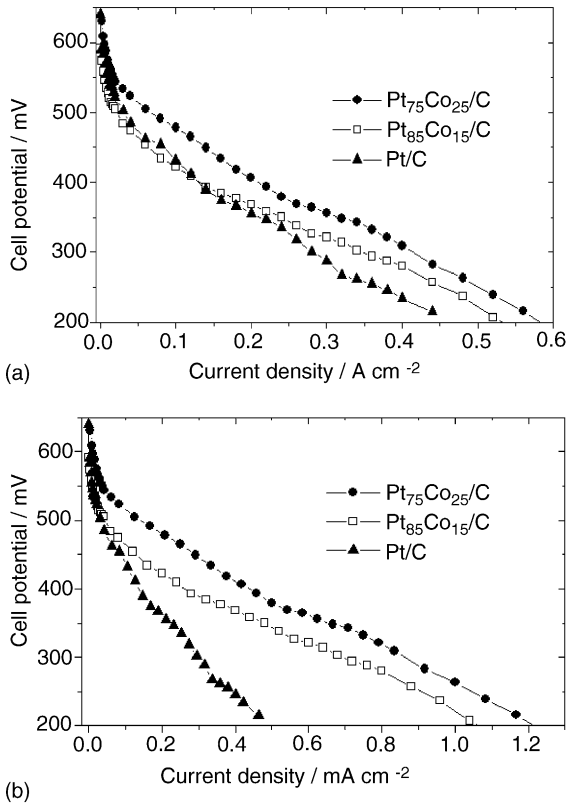

Fig. 9. Polarization curves in single DMFC with Pt–Co/C and Pt/C electrocatalysts for oxygen reduction at 90 °C and 3 atm O_2 pressure using a 2 mol L^{-1} methanol solution. Anode $Pt_{80}Ru_{20}$/C. (a) Current densities normalized with respect to the geometric surface area (MA); (b) current densities normalized with respect to the Pt surface area (SA).

4. Conclusions

The following conclusions can be drawn from this investigation:

- Carbon supported Pt–Co/C alloy electrocatalysts possess enhanced oxygen-reduction activity compared to Pt/C in the presence of methanol both in sulphuric acid electrolyte and in a single DMFC.
- A cobalt atomic fraction of 0.15 seems to be enough to improve the methanol tolerance of these binary electrocatalysts.
- The high methanol tolerance of Pt–Co/C electrocatalyts during the ORR is ascribed to the low activity of the binary electrocatalysts for methanol oxidation, arising from a composition effect.

Acknowledgements

The authors thank. the Conselho Nacional de Desenvolvimento Científico e Tecnológico (CNPq, Proc. 140205/2001-2) and the Fundação de Amparo a Pesquisa do Estado de São Paulo (FAPESP, Proc. 99/06430-8 and Proc. 03/04334-9) for financial assistance to the project. Thanks are also due to the Synchrotron Light Brazilian Laboratory (LNLS–Campinas, SP, Brazil) for assisting with the TEM experiments.

References

[1] X. Ren, P. Zelenay, S. Thomas, J. Davey, S. Gottesfeld, J. Power Sources 86 (2000) 111.
[2] J.-M. Léger, J. Appl. Electrochem. 31 (2001) 767.
[3] H.A. Gasteiger, N. Markovic, P.N. Ross, E.J. Cairns, J. Electrochem. Soc. 141 (1994) 1795.
[4] L. Dubau, C. Coutanceau, E. Garnier, J.-M. Léger, C. Lamy, J. Appl. Electrochem. 33 (2003) 419.
[5] R. Parsons, T. VanderNoot, J. Electroanal. Chem. 257 (1988) 9.
[6] S. Wasmus, A. Kuwer, J. Electroanal. Chem. 461 (1999) 14.
[7] B. Gurau, E.S. Smotkin, J. Power Sources 112 (2002) 3339.
[8] P.M. Urban, A. Funke, J.T. Muller, M. Himmen, A. Docter, Appl. Catal. A: Gen. 221 (2001) 459.
[9] A. Heinzel, V.M. Barragan, J. Power Sources 84 (1999) 70.
[10] K. Ramya, K.S. Dhathathreyan, J. Electroanal. Chem. 542 (2003) 109.
[11] J. Cruickshank, K. Scott, J. Power Sources 70 (1998) 40.
[12] B. Schubert, H. Tributsch, N. Alonso-Vante, A. Perrin, J. Catal. 112 (1988) 384.
[13] B. Schubert, N. Alonso-Vante, E. Gocke, H. Tributsch, Ber. Bunsenges Phys. Chem. 92 (1988) 1279.
[14] N. Alonso-Vante, H. Tributsch, Nature 323 (1996) 431.
[15] T.J. Schmidt, U.A. Paulus, H.A. Gasteiger, N. Alonso-Vante, R.J. Behm, J. Electrochem. Soc 147 (2000) 2620.
[16] R. Jiang, D. Chu, J. Electrochem. Soc. 147 (2000) 4605.
[17] P. Convert, C. Coutanceau, P. Crouigneau, F. Gloaguen, C. Lamy, J. Appl. Electrochem. 31 (2001) 945.
[18] U.A. Paulus, G.G. Scherer, A. Wokaun, T.J. Schmidt, V. Stamenkovic, V. Radmilovic, N.M. Markovic, P.N. Ross, J. Phys. Chem. B 106 (2002) 4181.
[19] V. Jalan, E.J.J. Taylor, J. Electrochem. Soc. 130 (1983) 2299.
[20] M. Min, J. Cho, K. Cho, H. Kim, Electrochim. Acta 45 (2000) 4211.
[21] S. Mukerjee, S. Srinivasan, J. Electroanal. Chem. 357 (1993) 201.
[22] S. Mukerjee, S. Srinivasan, M.P. Soriaga, J. McBreen, J. Electrochem. Soc. 142 (1995) 1409.
[23] T. Toda, H. Igarashi, H. Uchida, M. Watanabe, J. Electrochem. Soc. 146 (1999) 3750.
[24] E. Antolini, R.R. Passos, E.A. Ticianelli, Electrochim. Acta 48 (2002) 263.
[25] G. Tamizhmari, G.A. Capuano, J. Electrochem. Soc. 141 (1994) 968.
[26] M.T. Paffett, G.J. Berry, S. Gottesfeld, J. Electrochem. Soc. 135 (1988) 1431.
[27] K.T. Kim, J.T. Hwang, Y.G. Kim, J.S. Chung, J. Electrochem. Soc. 140 (1993) 31.
[28] J.B. Goodenough, R. Manoharan, A.K. Shukla, K.V. Ramesh, Chem. Mater. 1 (1989) 391.
[29] T. Toda, H. Igarashi, M. Watanabe, J. Electroanal. Chem. 460 (1999) 258.
[30] M. Watanabe, K. Tsurumi, T. Mizukami, T. Nakamura, P. Stonehart, J. Electrochem. Soc. 141 (1994) 2659.
[31] A.K. Shukla, M. Neergat, P. Bera, V. Jayaram, M.S. Hegde, J. Electroanal. Chem. 504 (2001) 111.
[32] L. Xiong, A.M. Kannan, A. Manthiram, Electrochem. Commun. 4 (2002) 898.
[33] J.-F. Drillet, A. Ee, J. Friedemann, R. Kotz, B. Schnyder, V.M. Schmidt, Electrochim. Acta 47 (2002) 1983.
[34] H. Yang, N. Alonso-Vante, J.-M. Leger, C. Lamy, J. Phys. Chem. B 108 (2004) 1938.

[35] A.K. Shukla, R.K. Raman, N.A. Choudhury, K.R. Priolkar, P.R. Sarode, S. Emura, R. Kumashiro, J. Electroanal. Chem. 563 (2004) 181.
[36] M. Neergat, A.K. Shukla, K.S. Gandhi, J. Appl. Electrochem. 31 (2001) 373.
[37] B.E. Warren, X-ray Diffraction, Addison-Wesley, Reading, MA, 1969 .
[38] Y.P. Mascarenhas, J.M.V. Pinheiro, In Programa para Calculo de Parametro de Rede pelo Metodo de Minimos Quadrados, SBPC, 1985.
[39] V.A. Paganin, E.A. Ticianelli, E.R. Gonzalez, J. Appl. Electrochem. 26 (1996) 297.
[40] F. Maillard, M. Martin, F. Gloaguen, J.-M. Leger, Electrochim. Acta 47 (2002) 3431.
[41] C. Lamy, A. Lima, V. Le Rhun, C. Coutanceau, J.-M. Leger, J. Power Sources 105 (2002) 283.
[42] H.A. Gasteiger, N.M. Markovic, P.N. Ross, E.J. Cairns, Electrochim. Acta 39 (1994) 1825.
[43] N.M. Markovic, P.N. Ross, Surf. Sci. Rep. 45 (2002) 121.
[44] S. Mukerjee, J. McBreen, J. Electroanal. Chem. 448 (1998) 163.
[45] S. Mukerjee, S. Srinivasan, M.P. Soriaga, J. McBreen, J. Electrochem. Soc. 142 (1995) 1409.